

Inhibition enhances the coherence in the Jacobi neuronal model

*Original*

Inhibition enhances the coherence in the Jacobi neuronal model / D'Onofrio, G.; Lansky, P.; Tamborrino, M.. - In: CHAOS, SOLITONS AND FRACTALS. - ISSN 0960-0779. - 128:(2019), pp. 108-113. [10.1016/j.chaos.2019.07.040]

*Availability:*

This version is available at: 11583/2982957 since: 2023-10-11T16:28:55Z

*Publisher:*

Elsevier

*Published*

DOI:10.1016/j.chaos.2019.07.040

*Terms of use:*

This article is made available under terms and conditions as specified in the corresponding bibliographic description in the repository

*Publisher copyright*

Elsevier preprint/submitted version

Preprint (submitted version) of an article published in CHAOS, SOLITONS AND FRACTALS © 2019,  
<http://doi.org/10.1016/j.chaos.2019.07.040>

(Article begins on next page)

# Inhibition enhances the coherence in the Jacobi neuronal model

Giuseppe D’Onofrio<sup>a,\*</sup>, Petr Lansky<sup>b</sup>, Massimiliano Tamborrino<sup>c</sup>

<sup>a</sup>*Dipartimento di Matematica “G. Peano”, Università degli Studi di Torino, Via Carlo Alberto 10, 10123 Torino, Italy*

<sup>b</sup>*Institute of Physiology of the Czech Academy of Sciences, Videnska 1083, 14220 Prague 4, Czech Republic*

<sup>c</sup>*Johannes Kepler University Linz, Altenbergerstraße 69, 4040 Linz, Austria*

---

## Abstract

The output signal is examined for the Jacobi neuronal model which is characterized by input-dependent multiplicative noise. The dependence of the noise on the rate of inhibition turns out to be of primary importance to observe maxima both in the output firing rate and in the diffusion coefficient of the spike count and, simultaneously, a minimum in the coefficient of variation (Fano factor). Moreover, we observe that an increment of the rate of inhibition can increase the degree of coherence computed from the power spectrum. This means that inhibition can enhance the coherence and thus the information transmission between the input and the output in this neuronal model. Finally, we stress that the firing rate, the coefficient of variation and the diffusion coefficient of the spike count cannot be used as the only indicator of coherence resonance without considering the power spectrum.

*Keywords:* coherence resonance, signal-to-noise ratio, leaky integrate-and-fire neuron model, multiplicative noise

---

\*Corresponding author

*Email addresses:* [giuseppe.donofrio@unito.it](mailto:giuseppe.donofrio@unito.it) (Giuseppe D’Onofrio), [lansky@biomed.cas.cz](mailto:lansky@biomed.cas.cz) (Petr Lansky), [massimiliano.tamborrino@jku.at](mailto:massimiliano.tamborrino@jku.at) (Massimiliano Tamborrino)

## 1. Introduction

Nonlinear dynamical systems are often strongly influenced by different sources of noise. The response of these systems to random fluctuations is of great interest because, differently from the typical assumption that noise can hinder or deteriorate the signal transmission, it has been observed that noise can sometimes improve the information processing both in theoretical models and in experiments [1, 2, 3, 4, 5]. Mathematical models in neuroscience are one of the most prominent examples for which noise is of primary importance or even a part of the signal itself rather than a source of inefficiency and unpredictability. In this article, we contribute to the discussion on this topic by studying the effects of a multiplicative noise on the performance of a single neuronal model using an analytical approach.

Typical examples of investigating the effect of noise are numerous studies on so-called stochastic resonance [6, 7, 8, 9, 10]. Broadly speaking, stochastic resonance is observed when increasing the level of noise improves the signal transmission or detection performance, instead of deteriorating it. The term is traditionally reserved for studying periodic signals. However, it is also natural to ask whether the noise optimizes the information transmission via small aperiodic signals. Then, contrary to the usual setup of stochastic resonance, no external periodic driving is assumed and the coherence that appears as a nonlinear response of the system to the input signal or to a purely noisy excitation is called aperiodic resonance [11] or *coherence resonance* [12, 13, 14]. What happens is that for both small and large noise amplitudes, the noise-excited activity appears to be rather irregular, while for moderate noise relatively coherent outputs are observed. Then, the information on the input can be inferred from the available observation of the output. In case of an aperiodic input the word resonance can be misleading, so McDonnell and Ward [1] suggested using the term *stochastic facilitation*.

Several specific measures are employed to quantify the above mentioned effects of the noise. For example, the characteristic correlation time is used in

[13] for the FitzHugh-Nagumo model. Other examples are the cross-correlation coefficient,[11], for the integrate-and-fire or Hodgkin-Huxley neuron models or the mutual information between the input and the output, [15]. However, the most commonly used measures are evaluated from the power spectrum both for single neurons [12, 14, 16, 17, 18, 19, 20] and recently for neuronal networks [21, 22, 23]. The metric we use here as an indicator of the stochastic facilitation is the *degree of coherence*,  $\beta$ . It is based on the power spectrum and it is directly related to the Fisher information. In particular, using Shannon's formula, the total amount of information,  $I$ , contained in the neuronal output is proportional to a function of  $\beta$  (for details see [24])

$$I \propto \int \log_2[1 + \beta] d\omega.$$

The previous examples of stochastic resonance, coherence resonance or stochastic  
 30 facilitation are mostly based on manipulating the noise component of the system. However, neurons and consequently their models are characterized by the rather intuitive property that the noise amplitude is signal dependent [3, 25, 26, 27, 28]. The signal is composed of excitation and inhibition and it is not so intuitive that despite the integrated level of the signal (sum of excitation  
 35 and inhibition) is kept constant, due to the manipulation with its components, the noise can be attenuated or enhanced. This may lead to seemingly paradoxical results and the mechanism is also used here. We analyze the dependence of the output on the rate of inhibitory inputs, showing that a small contribution of inhibition can enhance the degree of coherence and thus improve the coding  
 40 performance. The employed model is based on the Jacobi diffusion [29] and it represents a good compromise between mathematical tractability and biological accuracy. For the considered model, in [30] it is shown that the dependence of the parameters on the rate of inhibition is of primary importance to observe a change in the slope of the response curves. This dependence also affects the  
 45 variability of the output as reflected by the coefficient of variation, which often takes values larger than one and is not always a monotonic function of the rate of excitation.

The paper is organized as follows. We summarize the Jacobi neuronal model and we recall relevant mathematical tools in Section 2. The measures of coherence are listed together with their interpretation and relation with the statistical moments of the first-passage time in Section 3. These methods of coherence quantification are used to obtain the main results in Section 4 and are then discussed in Section 5.

## 2. The Jacobi neuronal model

The Jacobi neuronal model,  $X_t$ , describes the evolution of the neuronal membrane depolarization between two consecutive spikes and is defined by the following stochastic differential equation [30], [31], [32]

$$dX_t = \left( -\frac{X_t}{\tau} + \mu(V_E - X_t) + \nu(X_t - V_I) \right) dt + \sigma \sqrt{(V_E - X_t)(X_t - V_I)} dW_t, \quad (1)$$

where  $X_0 = 0$  and  $\tau > 0$  is the membrane time constant taking into account the spontaneous voltage decay toward the resting potential (set equal to zero here) in the absence of inputs,  $\mu$  and  $\nu$ . The two constants  $V_I < 0 < V_E$  are the inhibitory and excitatory reversal potentials, respectively. Here  $W_t$  is a standard Wiener process and the diffusion coefficient  $\sigma > 0$  controls the amplitude of the noise. Eq.(1) is obtained in [33] as a diffusion approximation of a Stein's model with reversal potentials. In that model two independent homogeneous Poisson processes represent the excitatory and inhibitory neuronal inputs, with intensities  $\lambda_E$  and  $\lambda_I$ , respectively. They describe the arrival of excitatory and inhibitory postsynaptic potentials and are such that the input parameters are

$$\mu = e\lambda_E, \quad \nu = i\lambda_I, \quad (2)$$

where  $i$  and  $e$  are constants such that  $-1 < i < 0 < e < 1$ . The square of the noise amplitude,  $\sigma^2$ , is assumed to depend linearly on the input rates through a constant  $\epsilon > 0$  in the following way

$$\sigma^2 = (\lambda_E + \lambda_I)\epsilon. \quad (3)$$

Relations (2) and (3) connect the mathematically tractable but abstract description (1), to more biophysical based models such as Stein's model [34, 35, 36] or conductance-based models [37, 38, 39]. It is obvious from Eqs. (2) and (3) that with increased input the noise amplitude also increases. In addition, combined with Eq.(1), it implies that the effect of the input is state-dependent, i.e., changes in the depolarization decrease if  $X_t$  approaches  $V_I$  or  $V_E$ , and that the process is confined in the interval  $(V_I, V_E)$ . Throughout the paper, the underlying parameters are chosen to meet the following condition

$$\frac{\sigma^2}{2} \leq \min \left( \mu - \frac{V_I}{\tau(V_E - V_I)}, \frac{V_E}{\tau(V_E - V_I)} - \nu \right), \quad (4)$$

55 that guarantees that both  $V_I$  and  $V_E$  are entrance boundaries, i.e., the process  $X_t$  cannot reach them in finite time.

To simplify the notation for further calculations, it is convenient to rescale the process  $X_t$  to the interval  $(0, 1)$ . Using the transformation  $y = \frac{x - V_I}{V_E - V_I}$  in Eq.(1), we obtain

$$dY_t = (-aY_t + b)dt + \sigma\sqrt{Y_t(1 - Y_t)}dW_t, \quad Y_0 = y_0, \quad (5)$$

with

$$a = \frac{1}{\tau} + \mu - \nu, \quad b = \mu - \frac{V_I}{\tau(V_E - V_I)}, \quad y_0 = -\frac{V_I}{V_E - V_I}. \quad (6)$$

In accordance with the model, spikes of the neuron under study are generated when the process  $Y_t$  crosses a voltage threshold  $S = \frac{S_0 - V_I}{V_E - V_I}$ , with  $V_I < 0 < S_0 < V_E$  and  $0 < y_0 < S < 1$  for the first time, the so-called first-passage time (FPT). After a spike, the process is reset to the starting point  $y_0$  and the evolution starts anew. This reset condition introduces a nonlinearity in the dynamics and guarantees that the interspike intervals (ISIs) form a renewal process. In this case, the ISIs are independent and identically distributed as the FPT, denoted here by  $T$  and defined as

$$T := \inf\{t \geq 0 : Y_t \geq S | 0 < y_0 < S < 1\} = \inf\{t \geq 0 : X_t \geq S_0 | V_I < 0 < S_0 < V_E\},$$

with probability density function  $g(t)$ . The Laplace transform of  $T$ , i.e.,  $g^*(\xi) := \mathbb{E}[e^{-\xi T}] = \int_0^\infty e^{-\xi t} g(t) dt, \xi > 0$ , is used to calculate the moments of  $T$  and the

power spectral density, and is given by [31]

$$g^*(\xi) = \frac{{}_2F_1(k(\xi), \theta(\xi); \gamma; y_0)}{{}_2F_1(k(\xi), \theta(\xi), \gamma; S)}, \quad (7)$$

where

$$k(\xi) = \frac{2\xi}{\theta\sigma^2}, \quad \theta(\xi) = \frac{2a - \sigma^2 - \sqrt{(\sigma^2 - 2a)^2 - 8\xi\sigma^2}}{2\sigma^2}, \quad \gamma = \frac{2b}{\sigma^2},$$

and  ${}_2F_1$  denotes the Gaussian hypergeometric function. Note that, since  $S_0 < V_E$ , only the condition  $\sigma^2 \leq 2\mu - 2V_I/(\tau(V_E - V_I))$  for  $V_I$  to be entrance boundary is needed.

### 60 3. Methods for coherence quantification

Common quantities used in the studies on neuronal firing activity are the firing rate and the variability of the ISIs. The firing rate,  $f$ , is usually defined as the inverse of the mean FPT, i.e.  $f = 1/\mathbb{E}(T)$  [40]. The variability is often characterized by the coefficient of variation of  $T$ , CV, that is the ratio between the standard deviation and the mean of  $T$ , i.e.,  $\text{CV} = \sqrt{\text{Var}(T)}/\mathbb{E}(T)$ . The quantity  $(\text{CV})^2$  is equal to the Fano factor [41, 42, 43] (also called index of dispersion) for a renewal process. The presence of coherence resonance is often investigated by only looking at the behavior of the CV [13, 44, 45], without relying on other coefficients. In addition to these quantities, we recall the definition of the (effective) diffusion coefficient of the spike count,  $D_{\text{eff}}$ , [41]. For a renewal process, it can be expressed by the moments of  $T$ , namely [2, 19]

$$D_{\text{eff}} = \frac{1}{2} \frac{\text{Var}(T)}{\mathbb{E}(T)^3} = \frac{1}{2} (\text{CV})^2 f. \quad (8)$$

It determines how fast the variance of  $T$  grows with respect to the cube of the mean of  $T$ .

One of the methods to detect the presence of coherence is the analysis of the power spectral density given by

$$S(\omega) = \frac{1 - |\rho(\omega)|^2}{|1 - \rho(\omega)|^2} f, \quad (9)$$

where  $\rho(\omega)$  is the Fourier transform of the ISI density function,  $g(t)$ . The spectrum at vanishing and infinite frequency is related to the above quantities as follows, [18]

$$\lim_{\omega \rightarrow 0} S(\omega) = 2D_{\text{eff}} = (CV)^2 f, \quad \lim_{\omega \rightarrow \infty} S(\omega) = f. \quad (10)$$

The neuron may possess a noise-induced eigenfrequency, which appears as a peak in the spectrum, meaning that there is a preferred frequency. We denote by  $S(\omega_{\text{max}})$  the value of the peak in the power spectrum, by  $2h$  the height of the peak over  $f$ , i.e.,  $2h := S(\omega_{\text{max}}) - f$  and by  $S_h$  the value at the half height  $h$  of the peak over  $f$ , i.e.,  $S_h := f + h = S(\omega_{\text{max}}) - h = [S(\omega_{\text{max}}) + f]/2$ , see Fig.1. The size of the peak can be quantified by the degree of coherence,  $\beta$ , which is the ratio of peak height to the relative width with respect to the position of the maximum  $\omega_{\text{max}}$  of the power spectrum [17]. Here we choose the width at one half of the peak height over  $f$ , i.e.,  $S_h$ , as in [18] (see Fig.1). So we use the following version of the degree of coherence

$$\beta = \frac{S(\omega_{\text{max}}) - f}{\omega_2 - \omega_1} \omega_{\text{max}}, \quad (11)$$

where

$$\omega_1 = \min_{\omega_{\text{min}} \leq \omega \leq \omega_{\text{max}}} \{S(\omega) \geq S_h\}, \quad \omega_2 = \max_{\omega \geq \omega_{\text{max}}} \{S(\omega) \geq S_h\}.$$

The spectrum at vanishing frequencies is either below or above  $f$  depending on  
65 whether the CV is smaller or larger than one, respectively, cf. Eq.(10). As a  
consequence,  $S(\omega)$  can be bigger than  $S(\omega_{\text{max}})$  for  $\omega \approx 0$  if  $CV > 1$ . By setting  
 $\omega_{\text{min}}$  to 0 when  $CV < 1$  or to the frequency at which a local minimum  $S(\omega_{\text{min}}) <$   
 $f$  is observed when  $CV > 1$ , we guarantee that  $S(\omega_{\text{max}})$  is the global maximum  
of the power spectrum in  $[\omega_{\text{min}}, \infty)$ , avoiding possible numerical maximization  
70 problems. An illustration of all quantities of interest entering in (11) is given  
in Fig. 1. The degree of coherence (11) often goes under the name of signal-to-  
noise ratio (SNR)[12], or coherent SNR [14], that measures how well a spectral  
peak is expressed with respect to the value of the background noise [2].



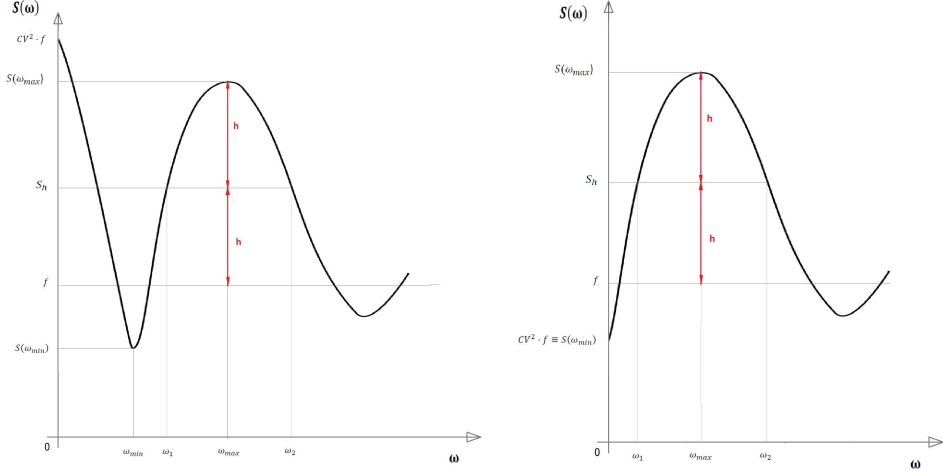


Figure 1: Illustration of the quantities defined in Eq.(11). The firing rate  $f$  is the high-frequency limit of the power spectrum, cf. Eq.(10), which has its highest peak in  $\omega_{\max}$ . The height of the peak over  $f$  is  $2h$ , i.e.,  $2h = S(\omega_{\max}) - f$ , while  $S_h$  denotes the value at the half of the height of the peak over  $f$ , i.e.,  $S_h = f + h = S(\omega_{\max}) - h$ . When  $CV > 1$ ,  $\omega_{\min}$  is the frequency at which a local minimum  $S(\omega_{\min}) < f$  is observed (left panel). When  $CV < 1$ , we set  $\omega_{\min}$  to zero (right panel). This guarantees that the peak  $S(\omega_{\max})$  is the global maximum of the spectrum in  $[\omega_{\min}, \infty)$ .

#### 4. Results

75 We analyze the above quantitative measures of neuronal firing for the Jacobi model (1) in dependence on the rate of the inhibitory input,  $\lambda_I$ . Due to the interrelationship among the parameters in Eqs.(1)-(3), some counterintuitive effects are observed. The firing rate,  $f$ , the coefficient of variation,  $CV$ , and the diffusion coefficient,  $D_{\text{eff}}$ , are shown in Fig.2 as a function of  $\lambda_I$ , for different  
80 values of the excitatory rate,  $\lambda_E$ . The firing rate is not always decreasing for increasing inhibition. For small values of  $\lambda_E$  it can increase with  $\lambda_I$  as a result of the form of the noise (cf. Eq.(2); a detailed discussion is given in Ref.[30]). We note that the CVs show minima for two of the curves for  $\lambda_I$  smaller than  $0.5 \text{ ms}^{-1}$ . They attain values above 1 for  $\lambda_I$  larger than  $0.5 \text{ ms}^{-1}$ . The behavior

85 of  $D_{\text{eff}}$  is similar to that of  $f$  because, for the selected parameters,  $\text{CV} \approx 1$  (cf. Eq.(8)). For values of  $\lambda_I$  and  $\lambda_E$  close to zero,  $D_{\text{eff}}$  is almost zero because the neuron is practically silent.

The  $D_{\text{eff}}$  achieves a maximum for small values of the excitatory rate ( $\lambda_E \leq 0.15$   $\text{ms}^{-1}$ ) but with  $\lambda_I$  strong enough to produce spikes. For stronger inhibitory  
90 inputs the diffusion coefficient decreases, meaning that the CV is relatively stable with respect to the firing rate.

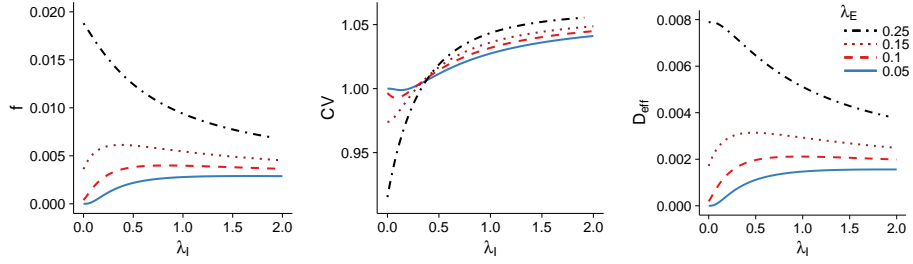


Figure 2: The firing rate, the coefficient of variation of the interspike intervals and the diffusion coefficient of the spike count for the Jacobi neuronal model (1) as a function of the inhibitory rate,  $\lambda_I$ , for different values of the excitatory inputs rate,  $\lambda_E$  (in the legends). The values of the other parameters are chosen as in Ref.[31] :  $S_0 = 10$  mV,  $x_0 = 0$  mV,  $V_I = -10$  mV,  $V_E = 100$  mV,  $e = 0.02$ ,  $i = -0.2$ ,  $\tau = 5.8$  ms and  $\epsilon = 0.0145$ .

Evaluating the Laplace transform in Eq.(7) with imaginary argument  $\xi = 2\pi i\omega$ , from Eq.(9) we get the following formula for the power spectrum

$$S(\omega) = \frac{1}{\mathbb{E}(T)} \frac{|{}_2F_1(k(2\pi if), \theta(2\pi if); \gamma; S)|^2 - |{}_2F_1(k(2\pi if), \theta(2\pi if); \gamma; y_0)|^2}{|{}_2F_1(k(2\pi if), \theta(2\pi if); \gamma; S) - {}_2F_1(k(2\pi if), \theta(2\pi if); \gamma; y_0)|^2}. \quad (12)$$

Eq.(12) is implemented numerically in the computing environment R [46]. We show the shifted power spectra,  $S(\omega) - f$ , to emphasize the height of the peaks in Fig.3. We again choose  $\epsilon = 0.0145$ ,  $\tau = 5.8$  ms as in [31], and additionally  
95  $\epsilon = 0.025$ ,  $\tau = 3$  ms, values also in the physiological range and satisfying Eq.(4).

The power spectrum shows sharp peaks as a sign of coherence. In both cases, for increasing values of  $\lambda_I$  (from left to right in the figures), the peaks become higher (thus  $S(\omega_{\text{max}}) - f$  increases) and more peaked (thus  $\omega_2 - \omega_1$  decreases) up to a certain value of the inhibitory rate, and then they start to reduce their

100 amplitudes, suggesting the presence of a maximum in the degree of coherence  
 $\beta$ .

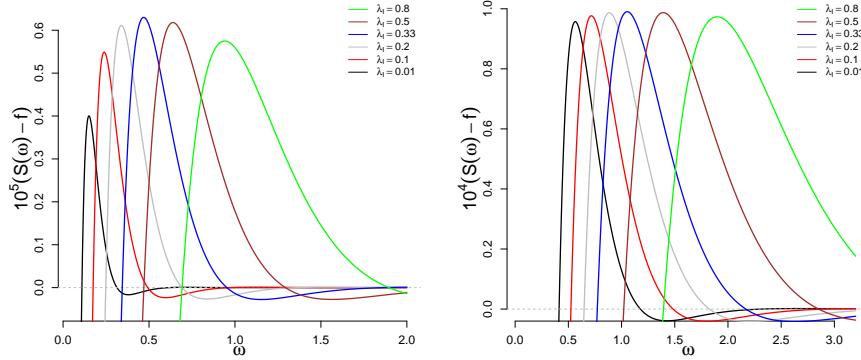


Figure 3: Rescaled power spectra of the Jacobi neuronal model from Eq.(9) for increasing values of  $\lambda_I$  (from left to right),  $\epsilon = 0.0145$ ,  $\lambda_E = 0.15 \text{ ms}^{-1}$ ,  $\tau = 5.8 \text{ ms}$  (left);  $\epsilon = 0.025$ ,  $\lambda_E = 0.34 \text{ ms}^{-1}$ ,  $\tau = 3 \text{ ms}$  (right). The other parameters are the same as in Fig.2. Peaks in correspondence of certain frequencies are clearly visible. The peaks become higher for increasing values of  $\lambda_I$  up to  $\lambda_I \approx 0.33 \text{ ms}^{-1}$  (and thus the degree of coherence  $\beta$  increases) and after that, their height decreases and their width increases (and thus  $\beta$  decreases), suggesting the presence of a maximum in  $\beta$ .

Increasing the excitatory rate increases generally the coherence of the spike train [2]. The same happens for the Jacobi model (figure not shown). The results are typically the opposite for increasing inhibitory inputs, for which the  
 105 corresponding neuronal output exhibits a decreased coherence. The degree of coherence of the Jacobi neuronal model as a function of  $\lambda_I$  is shown in Fig.4. Here, for relatively small values of the excitatory rate ( $\lambda_E = 0.15 \text{ ms}^{-1}$  or  $\lambda_E = 0.34 \text{ ms}^{-1}$ ), the inhibition increases the degree of coherence. We observe its maximum in the classical bell-shape of the SNR, typical of stochastic resonance.

110 Finally we notice that enhanced coherence is achieved for values of the parameters for which the  $D_{\text{eff}}$  shows a maximum, see for instance Fig.2 (right panel) and Fig.4 (left panel). The same effect is observed for  $\epsilon = 0.025$  (figure not shown).

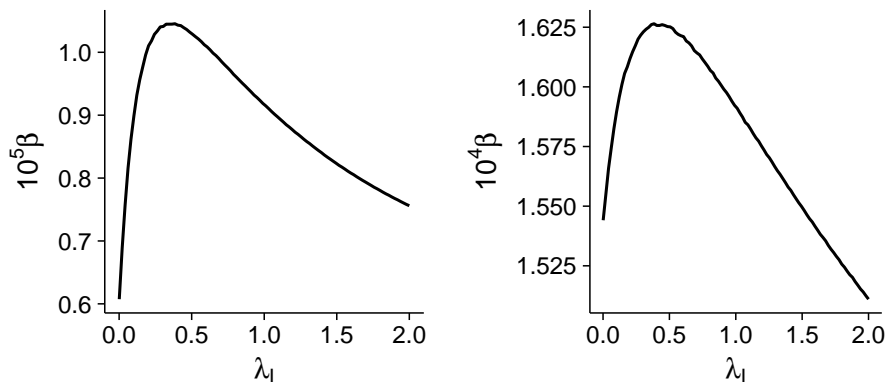


Figure 4: Degree of coherence as a function of  $\lambda_I$  for  $\epsilon = 0.0145$ ,  $\lambda_E = 0.15 \text{ ms}^{-1}$ ,  $\tau = 5.8 \text{ ms}$  (left);  $\epsilon = 0.025$ ,  $\lambda_E = 0.34 \text{ ms}^{-1}$ ,  $\tau = 3 \text{ ms}$  (right). The other parameters are the same as in Fig.2. For  $\lambda_I > 0.5 \text{ ms}^{-1}$  we observe the classical result: the coherence decreases for increasing inhibition. For  $\lambda_I < 0.5 \text{ ms}^{-1}$  and for relatively small values of the rate of arrival of excitatory inputs, the inhibition can increase the degree of coherence (even if the increment is small in terms of absolute values). We see that the coherence can be maximized by an optimum value of the inhibitory input rate (in this particular case around  $0.5 \text{ ms}^{-1}$ ). The lines are not straight due to small numerical errors in the evaluation of the power spectrum. We choose small  $\lambda_E$  because we want weak signals and the input  $b$  depends linearly on  $\lambda_E$  (see Eq.(6)).

## 5. Discussion

115 At low noise intensities and not sufficient excitation to evoke a spike, the membrane depolarization evolves mainly around the resting potential, with an occasional threshold crossing. Conversely, at large noise regimes, the membrane voltage fluctuations are dominated by the noise, the firings are frequent and highly irregular. Coherence resonance refers to the phenomenon that occurs  
120 at intermediate intensities of the noise and for which the firings become more regular than at low and high noise intensity scenarios [9, 13, 16, 17]. In the case of the Jacobi neuronal model, the square of the amplitude of the noise depends linearly on the input rates [30, 31, 32], so the approach presented in this paper is in the style of coherence resonance, but conceptually different. Instead of  
125 increasing the noise in presence of a weak signal, we increase the inhibitory rate,

$\lambda_I$ , affecting simultaneously the noise and the input  $\mu(V_E - X_t) + \nu(X_t - V_I)$ , cf. Eqs.(1)-(3), or, equivalently, looking at Eq.(5), we are manipulating also the coefficient that plays the role of the time constant through  $\nu$ .

In the presence of low excitation, the power spectrum of the Jacobi neuronal  
130 model is almost flat and it suggests that the firing activity is approximately  
Poissonian. However, we observe that an increment of the inhibitory rate can  
enhance the degree of coherence. Even if the effect is small in absolute value  
(the quantity  $S(\omega) - f$  is much smaller than  $f$ ), as far as we know, it has never  
been observed before. Another property of the Jacobi model discussed here  
135 concerns the diffusion coefficient,  $D_{\text{eff}}$ . It is a commonly accepted fact that  
the occurrence of a minimum in the diffusion coefficient vs noise intensity is a  
strong manifestation of coherence resonance [2, 18, 19]. In the case of the Jacobi  
neuronal model, enhanced coherence is observed for values of the parameters  
corresponding to a maximum in the diffusion coefficient vs inhibitory rate. This  
140 suggests that, as pointed out for the CV [2, 47], the presence of coherence  
resonance cannot be determined by only looking at  $D_{\text{eff}}$ .

These counter-intuitive results are consequences of the presence of reversal  
potentials in the model equation and we speculate that the same phenomena  
can be observed in other models with multiplicative noise, like the Feller or the  
145 inhomogeneous geometric Brownian motion [48]. The extension of these findings  
to the entire class of models with multiplicative noise will be the subject of future  
work.

## Acknowledgments

This work was supported by the Joint Research Project between Austria  
150 and the Czech Republic through Grant No. CZ 19/2019, by the Institute of  
Physiology RVO:67985823 and by the Czech Science Foundation project 17-  
06943S.

## References

- [1] M. D. McDonnell, L. M. Ward, The benefits of noise in neural systems: bridging theory and experiment, *Nature Reviews Neuroscience* 12 (10) (2011) 415–426. doi:10.1038/nrn3061.
- [2] B. Lindner, J. Garcia-Ojalvo, A. Neiman, L. Schimansky-Geier, Effects of noise in excitable systems, *Physics Reports* 392 (6) (2004) 321 – 424. doi:https://doi.org/10.1016/j.physrep.2003.10.015.
- [3] G. A. Cecchi, M. Sigman, J.-M. Alonso, L. Martínez, D. R. Chialvo, M. O. Magnasco, Noise in neurons is message dependent, *Proceedings of the National Academy of Sciences* 97 (10) (2000) 5557–5561. doi:10.1073/pnas.100113597.
- [4] M. Levakova, M. Tamborrino, L. Kostal, P. Lansky, Accuracy of rate coding: When shorter time window and higher spontaneous activity help, *Physical Review E* 95 (2017) 022310. doi:10.1103/PhysRevE.95.022310.
- [5] R. Naud, A. Payeur, A. Longtin, Noise gated by dendrosomatic interactions increases information transmission, *Physical Review X* 7 (2017) 031045. doi:10.1103/PhysRevX.7.031045.
- [6] M. D. McDonnell, D. Abbott, What is stochastic resonance? Definitions, misconceptions, debates, and its relevance to biology, *PLOS Computational Biology* 5 (5) (2009) 1–9. doi:10.1371/journal.pcbi.1000348.
- [7] R. Benzi, A. Sutera, A. Vulpiani, The mechanism of stochastic resonance, *Journal of Physics A: Mathematical and General* 14 (11) (1981) L453–L457. doi:10.1088/0305-4470/14/11/006.
- [8] P. Jung, P. Hänggi, Amplification of small signals via stochastic resonance, *Physical Review A* 44 (1991) 8032–8042. doi:10.1103/PhysRevA.44.8032.
- [9] L. Gammaitoni, P. Hänggi, P. Jung, F. Marchesoni, Stochastic resonance, *Review of Modern Physics* 70 (1998) 223–287. doi:10.1103/RevModPhys.70.223.

- [10] S. Herrmann, P. Imkeller, I. Pavlyukevich, D. Peithmann, Stochastic Resonance: A Mathematical Approach in the Small Noise Limit, Mathematical Surveys and Monographs, American Mathematical Society, 2013.
- [11] J. J. Collins, C. C. Chow, A. C. Capela, T. T. Imhoff, Aperiodic stochastic resonance, *Physical Review E* 54 (1996) 5575–5584. doi:10.1103/PhysRevE.54.5575.
- [12] H. Gang, T. Ditzinger, C. Z. Ning, H. Haken, Stochastic resonance without external periodic force, *Physical Review Letters* 71 (1993) 807–810. doi:10.1103/PhysRevLett.71.807.
- [13] A. S. Pikovsky, J. Kurths, Coherence resonance in a noise-driven excitable system, *Physical Review Letters* 78 (1997) 775–778. doi:10.1103/PhysRevLett.78.775.
- [14] S.-G. Lee, A. Neiman, S. Kim, Coherence resonance in a Hodgkin-Huxley neuron, *Physical Review E* 57 (1998) 3292–3297. doi:10.1103/PhysRevE.57.3292.
- [15] G. Deco, B. Schurmann, Stochastic resonance in the mutual information between input and output spike trains of noisy central neurons, *Physica D: Nonlinear Phenomena* 117 (1) (1998) 276 – 282. doi:https://doi.org/10.1016/S0167-2789(97)00313-8.
- [16] M. D. McDonnell, N. Iannella, M.-S. To, H. C. Tuckwell, J. Jost, B. S. Gutkin, L. M. Ward, A review of methods for identifying stochastic resonance in simulations of single neuron models, *Network: Computation in Neural Systems* 26 (2) (2015) 35–71. doi:10.3109/0954898X.2014.990064.
- [17] K. Pakdaman, S. Tanabe, T. Shimokawa, Coherence resonance and discharge time reliability in neurons and neuronal models, *Neural Networks* 14 (6) (2001) 895 – 905. doi:https://doi.org/10.1016/S0893-6080(01)00025-9.

- [18] B. Lindner, L. Schimansky-Geier, A. Longtin, Maximizing spike train coherence or incoherence in the leaky integrate-and-fire model, *Physical Review E* 66 (2002) 031916. doi:10.1103/PhysRevE.66.031916.
- [19] R. Guantes, G. G. de Polavieja, Variability in noise-driven integrator neurons, *Physical Review E* 71 (2005) 011911. doi:10.1103/PhysRevE.71.011911.
- [20] J. Bauermann, B. Lindner, Multiplicative noise is beneficial for the transmission of sensory signals in simple neuron models, *Biosystems* 178 (2019) 25–31. doi:doi.org/10.1016/j.biosystems.2019.02.002.
- [21] A. V. Andreev, V. V. Makarov, A. E. Runnova, A. N. Pisarchik, A. E. Hramov, Coherence resonance in stimulated neuronal network, *Chaos Solitons & Fractals* 106 (2018) 80 – 85. doi:doi.org/10.1016/j.chaos.2017.11.017.
- [22] K.-K. Wang, L. Ju, Y.-J. Wang, S.-H. Li, Impact of colored cross-correlated non-Gaussian and Gaussian noises on stochastic resonance and stochastic stability for a metapopulation system driven by a multiplicative signal, *Chaos, Solitons & Fractals* 108 (2018) 166 – 181. doi:https://doi.org/10.1016/j.chaos.2018.02.004.
- [23] H. Xie, Y. Gong, B. Wang, Spike-timing-dependent plasticity optimized coherence resonance and synchronization transitions by autaptic delay in adaptive scale-free neuronal networks, *Chaos, Solitons & Fractals* 108 (2018) 1 – 7. doi:https://doi.org/10.1016/j.chaos.2018.01.020.
- [24] M. Stemmler, A single spike suffices: the simplest form of stochastic resonance in model neurons, *Network: Computation in Neural Systems* 7 (4) (1996) 687–716. doi:10.1088/0954-898X74005.
- [25] A. A. Faisal, L. P. J. Selen, D. M. Wolpert, Noise in the nervous system, *Nature Reviews Neuroscience* 9 (4) (2008) 292–303. doi:https://doi.org/10.1038/nrn2258.



- [26] P. Lansky, L. Sacerdote, The Ornstein-Uhlenbeck neuronal model with signal-dependent noise, *Physics Letters A* 285 (3) (2001) 132–140. doi:  
[https://doi.org/10.1016/S0375-9601\(01\)00340-1](https://doi.org/10.1016/S0375-9601(01)00340-1).
- 240 [27] L. Sacerdote, P. Lansky, Interspike interval statistics in the Ornstein-Uhlenbeck neuronal model with signal-dependent noise, *Biosystems* 67 (1) (2002) 213 – 219. doi:  
[https://doi.org/10.1016/S0303-2647\(02\)00079-5](https://doi.org/10.1016/S0303-2647(02)00079-5).
- [28] P. E. Greenwood, P. Lansky, Optimum signal in a simple neuronal model with signal-dependent noise, *Biological Cybernetics* 92 (3) (2005) 199–205.  
245 doi:[10.1007/s00422-005-0545-3](https://doi.org/10.1007/s00422-005-0545-3).
- [29] S. Karlin, H. Taylor, *A Second Course in Stochastic Processes*, Academic Press, 1981.
- [30] G. D’Onofrio, M. Tamborrino, P. Lansky, The Jacobi diffusion process as a neuronal model, *Chaos: An Interdisciplinary Journal of Nonlinear Science* 28 (10) (2018) 103119. doi:  
250 [10.1063/1.5051494](https://doi.org/10.1063/1.5051494).
- [31] V. Lanska, P. Lansky, C. E. Smith, Synaptic transmission in a diffusion model for neural activity, *Journal of Theoretical Biology* 166 (4) (1994) 393 – 406. doi:  
<http://dx.doi.org/10.1006/jtbi.1994.1035>.
- 255 [32] A. Longtin, B. Doiron, A. R. Bulsara, Noise-induced divisive gain control in neuron models, *Biosystems* 67 (1) (2002) 147 – 156. doi:  
[https://doi.org/10.1016/S0303-2647\(02\)00073-4](https://doi.org/10.1016/S0303-2647(02)00073-4).
- [33] P. Lansky, V. Lanska, Diffusion approximation of the neuronal model with synaptic reversal potentials, *Biological Cybernetics* 56 (1) (1987) 19–26.  
260 doi:[10.1007/BF00333064](https://doi.org/10.1007/BF00333064).
- [34] R. B. Stein, A theoretical analysis of neuronal variability, *Biophysical Journal* 5 (2) (1965) 173 – 194. doi:  
[https://doi.org/10.1016/S0006-3495\(65\)86709-1](https://doi.org/10.1016/S0006-3495(65)86709-1).

- [35] H. Tuckwell, Introduction to Theoretical Neurobiology: Volume 2, Nonlinear and Stochastic Theories, Cambridge University Press, 2005.
- [36] M. Musila, P. Lansky, On the interspike intervals calculated from diffusion approximations of Stein's neuronal model with reversal potentials, *Journal of Theoretical Biology* 171 (2) (1994) 225 – 232. doi:<https://doi.org/10.1006/jtbi.1994.1226>.
- [37] M. J. E. Richardson, Effects of synaptic conductance on the voltage distribution and firing rate of spiking neurons, *Physical Review E* 69 (2004) 051918. doi:[10.1103/PhysRevE.69.051918](https://doi.org/10.1103/PhysRevE.69.051918).
- [38] S. Koyama, R. Kobayashi, Fluctuation scaling in neural spike trains, *Mathematical Biosciences and Engineering* 13 (2016) 537. doi:[10.3934/mbe.2016006](https://doi.org/10.3934/mbe.2016006).
- [39] R. Cofré, B. Cessac, Dynamics and spike trains statistics in conductance-based integrate-and-fire neural networks with chemical and electric synapses, *Chaos, Solitons & Fractals* 50 (2013) 13 – 31. doi:<https://doi.org/10.1016/j.chaos.2012.12.006>.
- [40] L. Kostal, P. Lansky, M. Stiber, Statistics of inverse interspike intervals: The instantaneous firing rate revisited, *Chaos: An Interdisciplinary Journal of Nonlinear Science* 28 (10) (2018) 106305. doi:[10.1063/1.5036831](https://doi.org/10.1063/1.5036831).
- [41] D. Cox, *Renewal Theory*, Methuen's monographs on applied probability and statistics, Methuen, 1962.
- [42] K. Rajdl, P. Lansky, Fano factor estimation, *Mathematical Biosciences & Engineering* 11 (2014) 105. doi:[10.3934/mbe.2014.11.105](https://doi.org/10.3934/mbe.2014.11.105).
- [43] R. Gusella, Characterizing the variability of arrival processes with indexes of dispersion, *IEEE Journal on Selected Areas in Communications* 9 (2) (1991) 203–211. doi:[10.1109/49.68448](https://doi.org/10.1109/49.68448).

- 290 [44] Y. Horikawa, Coherence resonance with multiple peaks in a coupled FitzHugh-Nagumo model, *Physical Review E* 64 (2001) 031905. doi:10.1103/PhysRevE.64.031905.
- [45] G.-Y. Zhong, H.-F. Li, J.-C. Li, D.-C. Mei, N.-S. Tang, C. Long, Coherence and anti-coherence resonance of corporation finance, *Chaos, Solitons & Fractals* 118 (2019) 376 – 385. doi:<https://doi.org/10.1016/j.chaos.2018.12.008>.  
295
- [46] R Core Team, *R: A Language and Environment for Statistical Computing*, R Foundation for Statistical Computing, Vienna, Austria (2013).  
URL <http://www.R-project.org/>
- 300 [47] J. W. Shuai, S. Zeng, P. Jung, Coherence resonance: On the use and abuse of the Fano factor, *Fluctuation and Noise Letters* 02 (03) (2002) L139–L146. doi:10.1142/S0219477502000749.
- [48] G. D’Onofrio, P. Lansky, E. Pirozzi, On two diffusion neuronal models with multiplicative noise: The mean first-passage time properties, *Chaos: An Interdisciplinary Journal of Nonlinear Science* 28 (4) (2018) 043103.  
305 doi:10.1063/1.5009574.